

## EVALUATING THE EFFECTIVENESS OF THE DTM SLOPE-BASED FILTER IN STRIPPING OFF ABOVE GROUND OBJECTS FROM DIGITAL AERIAL IMAGERY DSM IN RURAL LANDSCAPES

Fahmy F. F. Asal\*

Civil Engineering Department, Faculty of Engineering, Menoufia University, Egypt.

\*Correspondence: [fahmy.asal@sh-eng.menoufia.edu.eg](mailto:fahmy.asal@sh-eng.menoufia.edu.eg)

Citation:

F. F. F. Asal, "Evaluating the effectiveness of the DTM slope-based filter in stripping off above ground objects from digital aerial imagery DSM in rural landscapes". Journal of Al-Azhar University Engineering Sector, vol. 1, pp. 495 - 513, 2024.

Received: 6 January 2024

Revised: 20 February 2024

Accepted: 17 March 2024

DOI:10.21608/aej.2024.261004.1584

Copyright © 2024 by the authors. This article is an open-access article distributed under the terms and conditions of Creative Commons Attribution-Share Alike 4.0 International Public License (CC BY-SA 4.0)

### ABSTRACT

Generation of Digital Terrain Models (DTMs) in wide areas constitutes considerable challenges for base mapping. For DTM generation nonground cells have to be eliminated from Digital Surface Models (DSMs) through filtering processing of the DSMs. Different filtering approaches have been developed for surface smoothing and attenuation of the DSM high frequencies including the DTM slope-based filter. This research aimed at assessment of the efficiency of the DTM slope-based filter in stripping off nonground objects from digital aerial imagery DSMs in rural landscapes. The test site located at the west bank of a river at Vaihingen, Germany has a variety of rural landscape features where a DSM of 0.09-meter resolution extracted from digital aerial imagery stereo pairs has been employed in the study. Bare earth models and removed object layers created from filtering the DSM as well as closed gap bare earth models have been qualitatively and quantitatively analyzed along with accuracy estimation of the closed gap models. The analysis showed nodata gaps at the positions of the removed cells that increase in sizes with the increases in the filter radius. Also, the standard deviation of the bare model decreased by 12% with filter radius of 37 grid cells. However, with filter radius of 25 cells, the standard deviation of the elevation residuals increased by 1.53% while with filter radius of 29 cells that standard deviation increased by 13.62%. This indicates rapid deterioration in the accuracy the bare earth models created with filter radius greater than 25 grid cells.

**KEYWORDS:** Digital aerial imagery, DTM/DSM, Image matching, DTM slope-based filter, Roughness layers.

تقييم فعالية مرشح النماذج الأرضية الرقمية المعتمد على الميل في إزالة المعالم المنشأة فوق سطح الأرض الطبيعية من النماذج السطحية الرقمية المستخرجة من الصور الجوية الرقمية في المناطق الريفية

فهم عمل\*

قسم الهندسة المدنية، كلية الهندسة بشبين الكوم، جامعة المنوفية، مصر.

\*البريد الإلكتروني للباحث الرئيسي: [fahmy.asal@sh-eng.menoufia.edu.eg](mailto:fahmy.asal@sh-eng.menoufia.edu.eg)

الملخص

يشكل إنشاء النماذج الأرضية الرقمية (DTMs) في مناطق واسعة تحديات كبيرة لإنشاء خرائط الأساس. للحصول على DTM، يجب إزالة الخلايا غير الأرضية من النماذج السطحية الرقمية (DSMs) من خلال معالجة النصفية لـ DSMs. لقد تم تطوير أساليب ترشيح مختلفة لتنعيم السطح وتوهين ترددات DSM العالية بما في ذلك مرشح DTM المعتمد على الميل. يهدف هذا البحث إلى تقييم كفاءة مرشح DTM المعتمد على الميل في إزالة الأجسام غير الأرضية من DSMs المستخرجة من أزواج الصور الجوية الرقمية في المناطق الريفية. يحتوي موقع الاختبار الواقع على الضفة الغربية لنهر في فايهينجن بألمانيا على مجموعة متنوعة من المعالم وعناصر اللاندسكيب الريفية، حيث تم استخدام DSM بدقة 0.09 متر مستخرجة من أزواج الصور الجوية الرقمية

في الدراسة، حيث تم تحليل النماذج الأرضية المجردة وطبقات المعالم المزالة، والتي تم إنشاؤها من تصفية DSM بالإضافة إلى النماذج الأرضية المجردة المغلقة الفجوات نوعيًا وكميًا جنبًا إلى جنب مع تقدير الدقة للنماذج ذات الفجوات المغلقة. أظهر التحليل وجود فجوات في مواقع الخلايا الشبكية التي تمت إزالتها والتي تزداد أحجامها مع زيادة نصف قطر المرشح. كما انخفض الانحراف المعياري بنسبة 12% للنموذج الأرضي المجرد الناتج من استخدام مرشح ذي نصف قطر يبلغ 37 خلية شبكية. على العكس من ذلك، مع ازدياد نصف قطر المرشح إلى 25 خلية، زاد الانحراف المعياري لفروق المناسيب بنسبة 1.53% بينما مع ازدياد نصف قطر المرشح إلى 29 خلية شبكية زاد هذا الانحراف المعياري بنسبة 13.62% مما يشير إلى التدهور السريع في دقة النماذج الأرضية المجردة التي تم إنشاؤها بنصف قطر مرشح أكبر من 25 خلية شبكية.

**الكلمات المفتاحية:** الصور الجوية الرقمية، DTM/DSM، مطابقة الصور، مرشح DTM المعتمد على الميل، طبقات الحثونة الأرضية.

## 1. INTRODUCTION

A Digital Terrain Model (DTM) is a continuous surface depicts elevation values as the third dimension along with horizontal coordinates; northings and eastings in a rectangular cartesian coordinate system to determine the topography of the surface [1]. In other words, and due to the U.S. Geological Survey DTM is a cartographic representation of the land elevations at regularly spaced intervals in the x and y directions with the use of z-values referenced to a determined vertical datum. Therefore, a DTM represents the ground surface as bare earth [2]. In addition to elevations, the DTM contains other elements describing the topographic of the earth's surface such as the slope, the aspect, the curvature, the gradient, and others. Thus, for creation of a DTM from any discrete digital elevation datasets such datasets have to be taken on the ground surface and represent terrain elevations only [3, 4]. However, some digital elevation datasets including elevations of the surfaces of features such as trees, buildings, bridges, ...etc., might be used in creation of what is known as the Digital Surface Models (DSMs) where, a DSM is a continuous surface that depicts the elevations of the surfaces that are visible from the sensor, such as building tops, treetops, or unoccluded bare ground [5]. In this context, it is of immense importance to note here that filtering a DSM with specific filters of well-designed algorithms for separation of ground elevation areas from non-ground elevation features would result in a reliable DTM that can be employed in the analysis of different environmental and engineering aspects [6].

DSM has been a standard product from different aerial photography processing. The great developments in computing and electronics have had their effects on the aerial photography discipline leading to replacement of the former analogue and analytical photogrammetry with modern digital photogrammetry techniques and processing [7, 8]. In modern digital photogrammetry digital aerial cameras can capture aerial imagery with Ground Sampling Distance (GSD) that can be as small as a few centimeters. Additionally, the radiometric resolution given by modern digital aerial cameras is very high compared to what used to be provided by analogue aerial cameras. Identifying and measuring conjugate points in overlapped photographs is a fundamental photogrammetric operation. This operation is handled manually in analogue and analytical photogrammetry. Alternatively, in digital photogrammetry, image-matching techniques provide an automatic solution for such operations [9, 10]. Thus, the availability of high-quality digital images along with modern digital photogrammetry workstations has

provided means for automation of the different aspects of the photogrammetric problem including automation of DSM extraction and orthoimage generation [11, 12]. The automation procedures in digital photogrammetry for creation of DSMs depends on processing of digital image stereo pairs with the use of the digital image matching techniques also, known as image correlation. A digital image matching technique is mainly based on finding the conjugate pixel locations in two or more stereo pairs based on their geometric and radiometric characteristics [11, 13]. Thus, digital image matching processing of digital image stereo pairs gives 3D point cloud that can be subjected to an interpolation algorithm for creation of DSM [5, 14]. Different methods of image matching including area-based matching, feature based matching and relation or symbolic matching, can be distinguished [6, 15].

Creation of a reliable DTM constitutes a considerable challenge for base mapping especially in wide-area coverages since application of digital image matching techniques on digital image stereo pairs leads to extraction of DSMs with all man-made feature surface are represented in the DSM and missing of ground elevations in those areas [11, 16]. For removal of non-ground points from the aerial imagery DSM, the DSM has to be subjected for an efficient filtering processing to get a reliable DTM [1, 17]. Rokhmana, and Sastra, 2020 carried out research aimed at employment of an appropriate procedure method in Open-Source (OS) software for extraction of bare-earth model known as the DTM through filtering of available DSMs. They used SAGA-GIS open-source software for filtering a DSM generated from a Worldview-3 stereo ready images with the use of digital image matching techniques. Then, they carried out evaluation of quality of generated DTM from filtering operation of the DSM by visual interpretation through comparison with Worldview-3 orthoimage created with use of the same DSM. They recommended that good filtering operation can successfully strip off non-ground points from the DSM that can lead to creation of a high resolution DTM [1].

Krauß et al., 2011 state that application of DTM generation methods should restore the original ground model as accurate as possible where if the extracted DTM and stripped off man-made object are summed together this should lead to reconstruction of the original DSM. Since a DSM maps the surface of different objects on the ground however, a DTM maps the ground information only, a DTM can be extracted from a DSM through identifying and stripping off all man-made objects with filling these areas of the removed objects [17]. Different developed methods for DSM filtering use the characteristics of the objects to be stripped off the DSM [17]. Özcan et al., 2018 state that DTM generation from remote sensing data enjoys wide applications motivated by the increased sensor resolution [18]. They proposed a filtering and segmentation method for DSM that begins with extracting the DSM feature points to be employed in a probabilistic framework for extraction of a non-ground object probability map in spatial domain where

the mode of this map is used as seed points in a segmentation method basing on morphological processing leading to ground filtering and DTM generation. They tested that method on a DSM obtained from WorldView-2 stereo image pairs and compared the results with three different methods. They acknowledged that their proposed method can be employed for generation of a reliable DTM in addition to having advantages in terms of robustness in dealing with urban areas of different properties [18].

Arefi et al., 2011 state that an efficient filtering method should be independent of terrain, outliers or gross errors, interpolation errors as well as the size of the above ground objects. Different filtering techniques for extraction of DTMs from DSM have been introduced [19]. Also, Arefi et al., 2011 propose an algorithm for DTM generation from high resolution CARTOSAT-1 satellite images with the application of two major steps: The first step is generation of DSM from digital imagery stereo pairs through application of image registration, performing digital image matching with use of the dense matching algorithm, then finally performing an appropriate interpolation processing leading into a regular grid DSM. In the second step they applied a digital image filtering procedure on the generated DSM for removal of non-ground points and creation of a DTM [19]. Also, in the second step, they applied a classification for the generated DSM grid cells into ground and nonground regions with application of an algorithm motivated from gray-scale image reconstruction to suppress unwanted elevated grid cells. Also, they applied qualitative and quantitative evaluation on the created DTM through application of comparative studies on the extracted profiles from the DSM and the DTM. They acknowledged that their evaluation showed that the vast majority of nonground objects regardless of their size have been removed with the achievement of appropriate outcomes in hilly and smooth residential regions [19]. Also, Stereńczak et al., 2016 present a study that evaluates which combination of filtering and interpolation methods that can give the best DTM accuracy in very dense forest in mountainous areas in the Sudety mountains of south-western Poland where they produced about 100 DTMs for each filtering method and carried out analysis for the most-accurate six DTMs. They acknowledged that slope in addition to undergrowth vegetation constituted the most important factors that determine the DTM accuracy in dense mountain forests [2].

As stated before, aerial photogrammetry operation can provide elevation measurements on the top surface of the landscape including terrain areas, tops of buildings, tops of trees and other topographic above ground objects. Therefore, to extract a DTM from a DSM, all elevations do not represent bare ground have to be removed and all gaps have to be filled with new data or subjected to rigorous interpolation technique [20]. Höhle, 2010 investigated DTM generation in built-up areas from aerial imagery systems and presented filtering and classification approaches and carried out practical tests leading to obtained results of two tests of 16 cm and 17 cm in the standard deviation

with the use of large format images from 1000 m altitude [20]. Perko et al., 2015 proposes a filtering approach that focusses on robustness and computational efficiency to filter DSMs extracted from satellite stereo images for creation of a DTM. Their approach included integration of multi-directional processing and Slope Dependent (MSD) filtering to be known as MSD filtering where DTM extraction workflow is fully automatic [21]. They acknowledged that qualitative and quantitative evaluations of the created DTMs in comparison with high accuracy ground truth Light Detection and Ranging (LiDAR) data assures effectiveness of that method [21].

This research aims at evaluating the efficiency of the DTM slope-based filter in stripping off above ground objects from DSMs created from aerial imagery stereo pairs with the dense matching algorithms for creation of reliable DTMs in rural landscapes. Also, qualitative and quantitative analysis of the created DTMs constitute the main objectives of this research. Moreover, analysis of the extracted non-ground feature layers known as roughness layers is an important study objective.

## 2. THE DTM SLOPE-BASED FILTER

The slope-based filtering technique is one of the filters that is usually used for separating nonground points from ground points [19, 22]. In the slope-based filter the point is classified as ground point if there is no other point in its neighborhood to which the height difference is greater than a determined threshold. The slope-based filtering method assumes that the ground slopes are not greater a certain value where the features of slopes above that threshold are considered as nonground objects that need to be stripped off the DSM for creation of a DTM. This approach is much more suitable for gently slopped terrain regions [23]. Therefore, modifications have been carried to get a modified slope-based filtering basing on varying the threshold value that is determined by the terrain slopes where the filtering strategy is basing on iterative processing for trend elimination and linear prediction for stripping off nonground regions from the DSM [19].

The System for Automated Geoscientific Analysis (SAGA) is an open-source Geographic Information System (GIS) and image processing software that is used in this study. DTM slope-based filter is one of the many powerful filtering tools that can be run under SAGA. Wichmann, 2010 states that DTM slope-based filter can be used to filter a DSM to classify it into a bare earth layer and a removed object layer [24]. The bare earth layer can be called DTM layer as it contains ground elevation areas with removed non-ground areas left as gaps in the resulting bare earth model. On the other hand, the removed object layer contains areas of the features layers and can be known as non-ground feature layer. DTM slope-based filtering approach is based on a concept that assumes that a big elevation difference between two adjacent grid cells is unlikely to occur due to a steep slope in the ground surface [25, 26]. Therefore, the probability of the high

elevation grid cell being a ground point decreases if the distance between the two grid cells decreases. Additionally, the filter decides the acceptable height difference between the two grid cells as a function of the distance between them. Therefore, the grid cell is considered as ground if there is no grid cell within the search radius of the filter that the height difference between these grid cells is bigger than the allowed maximum height difference at the distance between these grid cells. Moreover, an approximate ground surface slope variable is employed to improve the filter function to suit the overall slope in the DSM. Furthermore, for removal of blunders, a confidence interval can be evaluated [24].

### 3. MATERIALS AND METHODS

The dataset employed in this investigation constitute a clipped part DSM in rural landscape of the whole DSM for Vaihingen city in Germany. The test DSM is of 0.09-meter ground resolution was generated from digital aerial imagery stereo pairs with the use of dense matching algorithm under the Match-T DSM module working under INPHO digital photogrammetry and image processing software and provided by the German Association of Photogrammetry and Remote Sensing (DGPF) who generated the DSM and the orthoimage of the test site at 0.09-meter ground resolution [27, 28]. The dataset represents a subset of large amount of test data exploited for testing of digital aerial cameras and was captured by the DGPF [29, 30]. Figure 1 illustrates an orthoimage of the test site located at Vaihingen city in Germany that was created by the same test DSM. The test site is located at the west bank of a river at Vaihingen city, Germany possesses varieties of rural landscape elements, as appear in the orthoimage, figure 1. This includes water areas and wide paved and green parks, in addition to rows of trees and multi bay business buildings. In carrying out of this research, bare earth models have been created as results of filtering the DSM resulting from image matching with the slope-based filter at varying kernel radii and have been visually and statistically analyzed. In addition, removed object models known as the roughness layers extracted as results of filtering of the image matching DSM with the slope-based filter at varying kernel radii have been presented and subjected to qualitative and quantitative assessment. Moreover, closed gap bare earth models have been generated with use of the spline interpolation methods and subjected to qualitative and quantitative evaluations as well. Finally, accuracy estimation of the closed gap bare earth models with employment of a handful of external ground truth data extracted from the provided LiDAR point clouds of the test site have been undertaken. Different image processing and GIS software including SAGA 9.3, Surfer 10, ESRI ArcView 3.3 and LAStools have been employed in the analysis.



**Fig. 1.** An ortho image of 0.09 meter ground resolution for the test site located at the west bank of the river in Vaihingen city, Germany.

## 4. RESULTS AND DISCUSSION

### 4.1. Analysis of the Created Bare Earth Models

**Fig. 2 (b - h)** depicts bare earth models extracted from an aerial imagery DSM of 0.09-meter ground resolution, **Fig. 2a** with the use of the DTM slope-based filter working under SAGA GIS software of varying kernel radii of 5, 9, 13, 17, 21, 25, 29 grid cells respectively. In **Fig. 2** the DTM slope-based filter of varying radii has stripped off varied amounts of the rural landscape leaving bare earth models that can be considered as DTMs of the test area. Clear gaps of no data have been left at the positions of the removed parts of the rural landscape. The amounts and sizes of the removed objects increase with the increase in the kernel radius of the DTM slope-based filter. Thus, the bare earth model in **Fig. 2b** records the smallest amounts of removed objects from the DSM with use of kernel radius of 5 grid cells. However, with increasing in the kernel radius size the amounts of the stripped objects increased. This is obvious in **Fig. 2h** which is a bare earth model where the DTM slope-based filter of kernel radius of 29 grid cells has removed the largest amounts of the rural landscape elements. This can be easily interpretable from the amounts and sizes of the no data gaps of white color found in the bare earth models in **Fig. 2 (b - h)**. **Table 1** shows the statistical analysis of results of the bare earth models created from the aerial imagery DSM, figure 2a with application of the DTM slope-based filter of varying kernel radii of 3, 5, 9, 13, 17, 21, 25, 29, 33, 37 grid cells in addition to the statistical analysis results of the original aerial imagery DSM in **Fig. 2a**. From **Table 1**, the DTM slope-based filter has kept the minimum elevation, the maximum elevation, and the range of elevations of the original DSM unchanged regardless of application of the filter with varying kernel radii. On the other hand, the number of the data cells, the mean elevation, the sum of elevations, the variance of elevations in addition to the standard deviation of bare earth elevations decrease with increasing the radius of the DTM slope-based filter as shown in **Table 1** and **Fig. 3**. From **Table 1** and **Fig. 3**, the number of the no data cells increases with increasing the radius of the slope-based filter which refers to

EVALUATING THE EFFECTIVENESS OF THE DTM SLOPE-BASED FILTER IN STRIPPING OFF ABOVE GROUND OBJECTS FROM DIGITAL AERIAL IMAGERY DSM IN RURAL LANDSCAPES

increasing in the amounts of the removed landscape elements. Also, from **Table 1** and **Fig. 3** the standard deviation of the bare earth model elevation has decreased by about 12% with the use of the DTM slope-based filter with kernel radius of 37 due to removal of parts of non-ground objects.

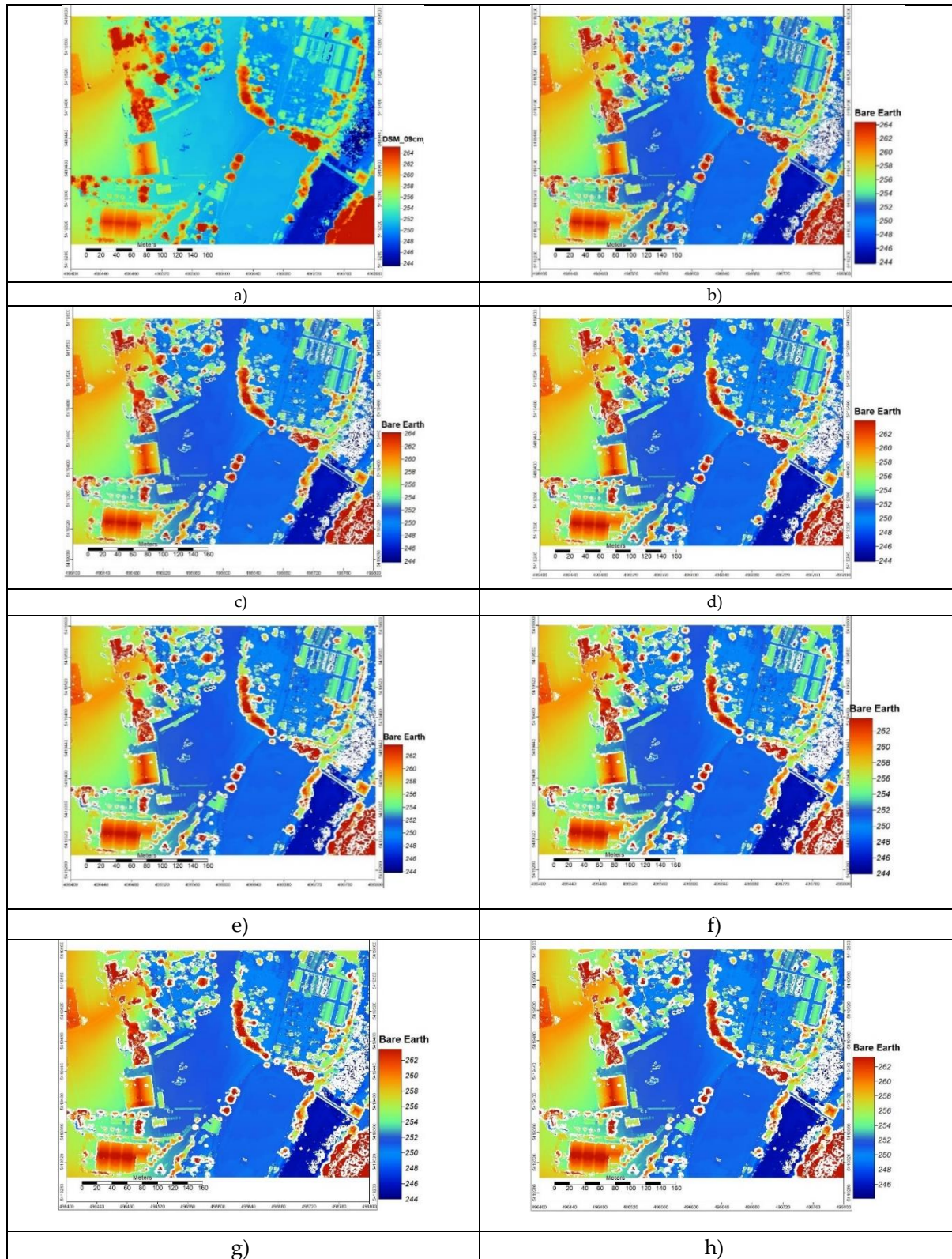


**Fig. 2.** a) Aerial imagery DSM and (b - h) bare earth models extracted through stripping off above ground objects from the DSM with the application of DTM slope-based filter of varying kernel radii of 5, 9, 13, 17, 21, 25 and 29 grid cells respectively.

**Table 1:** Statistical analysis results of bare-earth models created with the use of the DTM slope-based filter of varying kernel radii.

Bare Earth Model kernel radius (r)	Data Cells	No data Cells	Mean elev. (m.)	Min. elev. (meters)	Max. elevation (meters)	Range of elev. (meters)	Sum of elevations (meters)	Stand. dev. of elevation (meters)	Decrease in stand. dev. of elevation (%)
r=0	14822964	0	254.305	229.702	283.501	53.799	3.77E+09	5.409	0.000
r=3	13149836	1673128	254.111	229.702	283.501	53.799	3.34E+09	5.196	3.938
r=5	12922748	1900216	254.052	229.702	283.501	53.799	3.28E+09	5.155	4.696
r=9	12595428	2227536	253.952	229.702	283.501	53.799	3.2E+09	5.086	5.972
r=13	12390945	2432019	253.873	229.702	283.480	53.778	3.15E+09	5.023	7.136
r=17	12253936	2569028	253.809	229.702	283.303	53.600	3.11E+09	4.966	8.190
r=21	12161367	2661597	253.757	229.702	283.230	53.527	3.09E+09	4.914	9.151
r=25	12099377	2723587	253.714	229.702	283.230	53.527	3.07E+09	4.867	10.020
r=29	12055383	2767581	253.679	229.702	283.230	53.527	3.06E+09	4.826	10.778
r=33	12021809	2801155	253.650	229.702	283.230	53.527	3.05E+09	4.789	11.462
r=37	11997959	2825005	253.628	229.702	283.230	53.527	3.04E+09	4.759	12.017

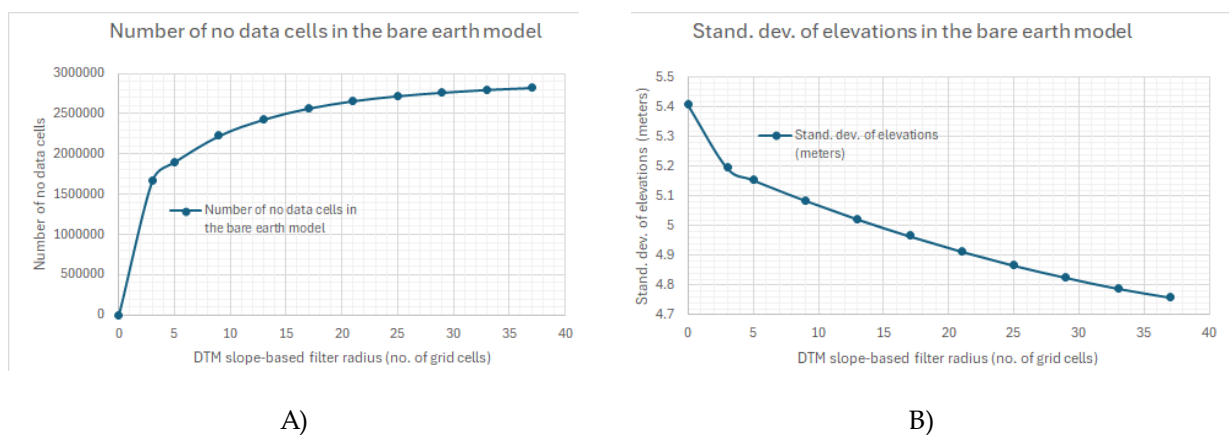


**Fig. 3.** A) Chart of the number of the no data cells in the bare earth models against the radius of the DTM slope-based filter, B) Chart of the standard deviation of the bare earth models against the size of the radius of the DTM slope-based filter.

#### 4.2. Evaluation of the Extracted Roughness Layers

Fig. 4 shows removed object models that represent non-ground feature layers and also can be known as the roughness layers. The roughness layers depict the removed non ground features due to filtering aerial imagery DSM of 0.09-meter resolutions with DTM slope-based filter of varying kernel radii as 3, 5, 9, 13, 17, 21, 25, 29 grid cells. In figures 4(a - h) the DTM slope-based filter has extracted above ground objects giving detailed feature layers with keeping the actual elevations of the tops of different features as they are in the original DSM. Also, in figures 4(a - h) the concentration and the amounts of the removed objects increase with increasing the radius of the DTM slope-based filter. Mainly the edges of features such as buildings and trees have been extracted as they are usually of high slope values that exceed the identified threshold slope value determined as the approximate value of the terrain slope by SAGA software.

EVALUATING THE EFFECTIVENESS OF THE DTM SLOPE-BASED FILTER IN STRIPPING OFF ABOVE GROUND OBJECTS FROM DIGITAL AERIAL IMAGERY DSM IN RURAL LANDSCAPES

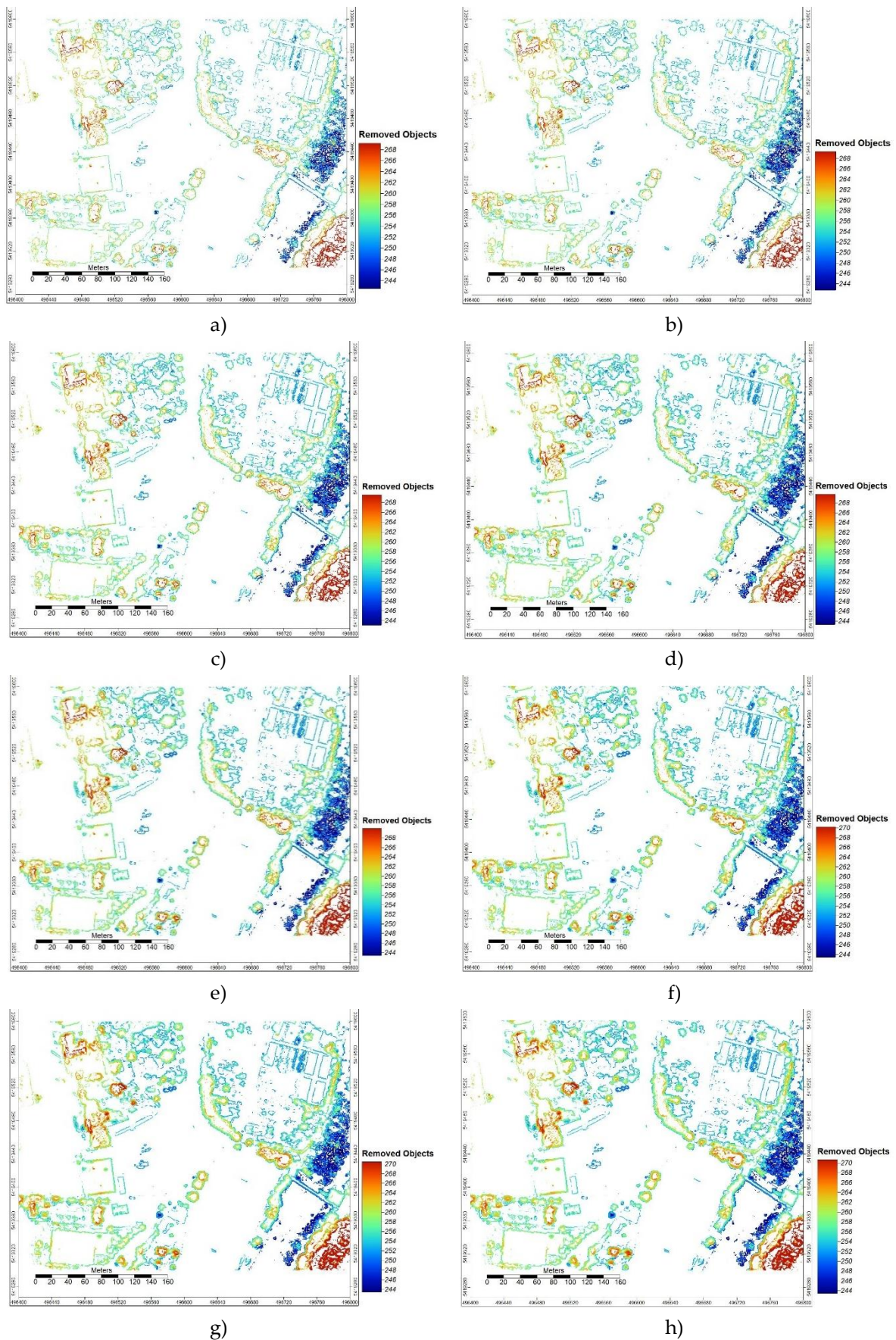


**Fig. 4.** (a - h) Roughness layers extracted through stripping off above ground features from aerial imagery DSM with the application of DTM slope-based filter of varying kernel radii of 3, 5, 9, 13, 17, 21, 25 and 29 grid cells respectively.

Table 2 shows the statistical analysis results of the removed object models known as the roughness layers that contain the removed above ground features from aerial imagery DSM with the use of the DTM slope-based filter of varying radii. Statistical analysis of the roughness layers indicates that the DTM slope-based filter keeps same minimum elevation in the different roughness layers regardless of increasing in the filter radius. On the other hand, the maximum elevation values of the roughness layers increase with increasing the radius of the DTM slope-based filter due to extraction of bigger amounts of the above ground features as the filter radius increases. This is reflected on increasing in the ranges of elevations, the mean elevations, the sum of elevations and the standard deviation of the elevations within the roughness layers which indicate that these statistical quantities increase with increasing the radius of the applied DTM slope-based filter on the aerial imagery DSM. This is also supported by increases in the numbers of the data cells and decreasing in the numbers of the no data cells due to increasing in the radius of the applied DTM slope-based filter which reflects increasing in removal of above ground features.

**Table 2:** Statistical analysis results of the roughness layers created with the use of the DTM slope-based filter of varying radii.

Removed object model filter radius (r)	Data Cells	No data Cells	Mean elev. (m.)	Min. elev. (m.)	Max. elev. (m.)	Range of elev. (m.)	Sum of elevations (meters)	Stand. dev. of elevations (meters)	Increase in stand. dev. of elevations (%)
r=3	1673142	13149822	255.825	230.147	283.115	52.968	4.28E+08	6.666	0.0
r=5	1900229	12922735	256.023	230.147	283.133	52.986	4.87E+08	6.640	-0.390
r=9	2227550	12595414	256.299	230.147	283.409	53.262	5.71E+08	6.613	-0.795
r=13	2432033	12390931	256.504	230.147	283.501	53.355	6.24E+08	6.631	-0.525
r=17	2569042	12253922	256.670	230.147	283.501	53.355	6.59E+08	6.664	-0.030
r=21	2661611	12161353	256.810	230.147	283.501	53.355	6.84E+08	6.704	0.570
r=25	2723601	12099363	256.930	230.147	283.501	53.355	7E+08	6.748	1.230
r=29	2767595	12055369	257.031	230.147	283.501	53.355	7.11E+08	6.799	1.995
r=33	2801169	12021795	257.114	230.147	283.501	53.355	7.2E+08	6.831	2.475
r=37	2825019	11997945	257.176	230.147	283.501	53.355	7.27E+08	6.865	2.985

#### 4.3. Analysis of the Closed Gap Bare Earth Models

As shown in Fig. 2 the created bare earth models from the application of the DTM slope-based filter of varying radius sizes on the aerial imagery DSM of 0.09-meter grid resolutions are full of no data gaps at the positions of the removed objects. These no data gaps affect the continuity of the DTMs and affect their employment as reliable DTMs in various applications. Therefore, it is necessary for the created bare earth models to be subjected to an interpolation operation to fill the gaps and obtain continuous surfaces representing the earth's surface as a reliable DTMs. In this analysis the created bare earth models in figures 2 have been subjected the tool called as "close the gaps with spline" under SAGA-GIS software package to fill all gaps in the created bare earth models and complement the process of obtaining continuous surface DTMs. Figure 5 depicts a group

of bare earth models extracted from aerial imagery DSM with the use of the DTM slope-based filter working under SAGA GIS software of kernel radii of 5, 9, 13, 17, 21, 25, 29 grid cells after filling the gap with the use of the “close the gaps with spline” tool under SAGA-GIS. From figures 5(a) to 5(h), with increasing in the DTM slope-based filter radius the different above ground features become thinner which refers to increasing in the amounts of removal of above ground features. Also, continuous surfaces have been obtained, however, even with the use of large DTM slope filter radius considerable amounts of above ground features yet to be removed. This reflects limitations of the DTM slope-based filter in removal of the tops of the features such as tops of the buildings and tops of trees which do not have as high slope values as the edges of the those features.

Table 3 shows the statistical analysis results of the closed gab bare earth models with application of the “close the gaps with spline” tool under SAGA-GIS. From table 3 the no data cells have become zero in all bare earth models due to successful closing of all the gaps. Also, the number of data cells have become the same in all the bare earth models. Additionally, the minimum elevation has been the same as the case before closing the gaps. However, the maximum elevation and the consequently the range of elevations have been decreasing with increasing the DTM slope-based filter radius after closing the gaps that can be due to smoothing of the surface implemented by the spline interpolation approach at wider gaps resulting from using larger filter radii. Also, decreases in the mean elevation as well as in the sum of elevations and in the standard deviation of elevations have been obtained due to increasing in the filter radius and the smoothing effects implemented by the spline approach.

EVALUATING THE EFFECTIVENESS OF THE DTM SLOPE-BASED FILTER IN STRIPPING OFF ABOVE GROUND OBJECTS FROM DIGITAL AERIAL IMAGERY DSM IN RURAL LANDSCAPES

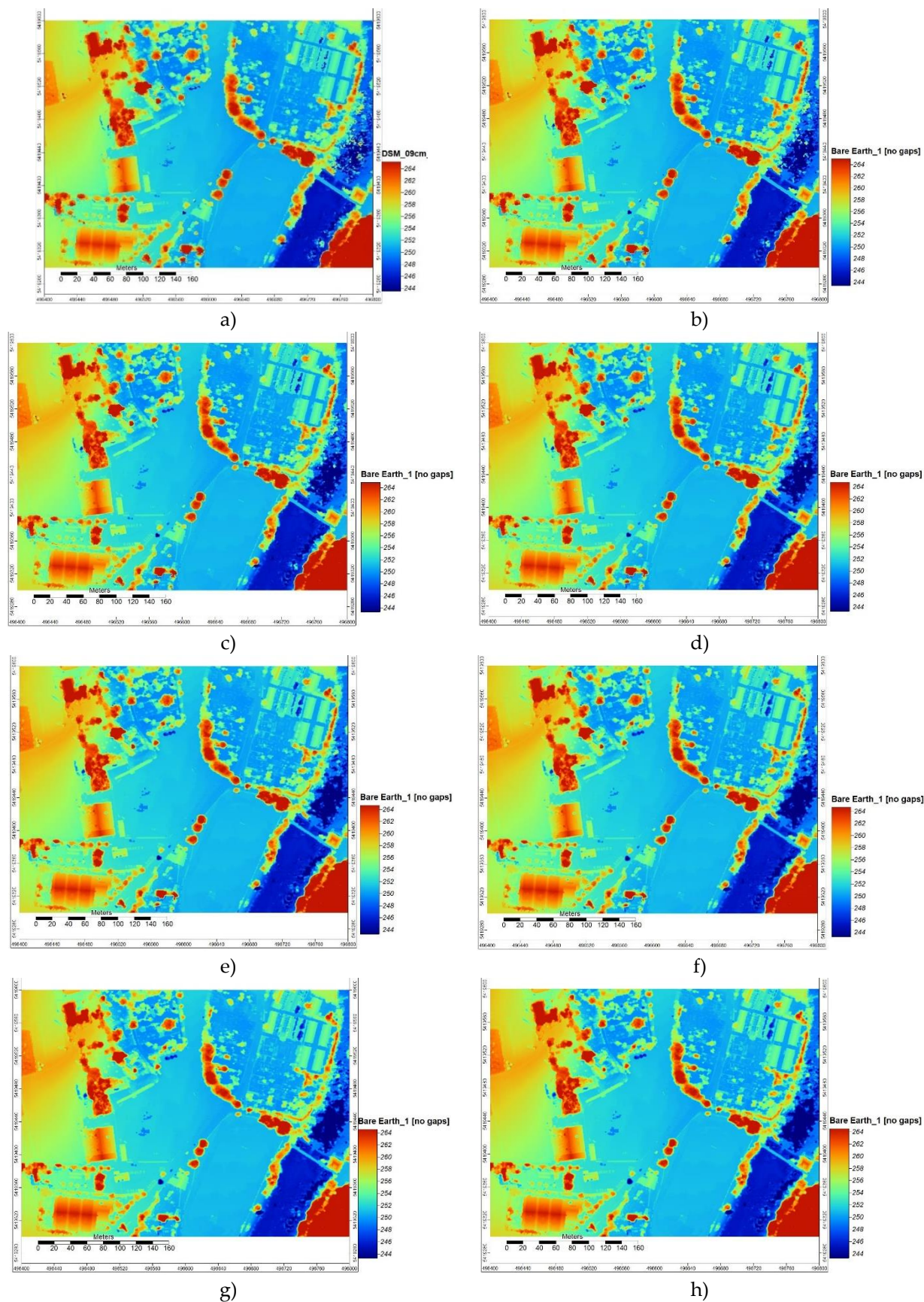


**Fig. 5.** a) Aerial imagery DSM and (b - h) closed gap bare earth models extracted through stripping off above ground objects from the DSM with the application of DTM slope-based filter of varying kernel radii of 5, 9, 13, 17, 21, 25 and 29 grid cells respectively and closing the gaps with application of the spline interpolation approach.

**Table 3:** statistical analysis results of the closed gap bare earth models with application of the “close the gaps with spline” tool under SAGA-GIS.

Bare earth model (no gaps) kernel radius (r)	Data Cells	Nodata Cells	Mean elev. (m.)	Min. elev. (m.)	Max. elev. (m.)	Range of elevations (meters)	Sum of elevations (meters)	Standard deviation of elevations (meters)	Decrease in the standard deviation of elevations (%)
r=0	14822964	0	254.305	229.702	283.501	53.799	3.77E+09	5.409	0
r=5	14822964	0	254.155	229.702	283.501	53.799	3.77E+09	5.399	0.184
r=9	14822964	0	254.072	229.702	283.501	53.799	3.77E+09	5.392	0.314
r=13	14822964	0	254.010	229.702	283.480	53.778	3.77E+09	5.380	0.536
r=17	14822964	0	253.961	229.702	283.303	53.600	3.76E+09	5.365	0.813
r=21	14822964	0	253.927	229.702	283.230	53.527	3.76E+09	5.349	1.109
r=25	14822964	0	253.898	229.702	283.230	53.527	3.76E+09	5.330	1.461
r=29	14822964	0	253.875	229.702	283.230	53.527	3.76E+09	5.312	1.793
r=33	14822964	0	253.855	229.702	283.230	53.527	3.76E+09	5.293	2.145
r=37	14822964	0	253.840	229.702	283.230	53.527	3.76E+09	5.276	2.459

#### 4.4. Accuracy Assessment of the Closed Gap Bare Earth Models

The closed gap bare earth models created from filtering of the aerial imagery DSM of 0.09-meter ground resolution with the DTM slope-based filter of varying radii and shown in figure 5 have been subjected to accuracy analysis in order to assess the accuracy of elevations extracted from these models. The methodology of this test is based on measuring point elevations from the different closed gap bare earth models at every position of some externally and precisely measured elevation checkpoints of ground truth elevation measurements. The differences between the elevations of the external checkpoints and the elevations extracted from the bare earth model at the same positions of the checkout point are calculated as residual elevations. Therefore, a similar number of elevation residuals to the number of checkpoints can be calculated and consequently statistically analyzed. Figure 6 shows a number of 263 external checkpoints that have been extracted from airborne laser scanning point clouds, accompanied with the test datasets and provided by German Society for Photogrammetry, Remote Sensing and Geoinformation (DGPF). The external checkpoints of this testing have been randomly extracted with the use of SAGA software to be exploited in the analysis. Figure 6 is a map that shows the random distribution of the extracted checkpoints from the provided airborne laser scanning point clouds at the test site area and viewed over the aerial image matching DSM of 0.090-meter ground resolution at rural landscape area. Additionally, the results of the statistical analysis of the calculated elevation residual are presented in table 4. Moreover, figure 7 presents two charts that provide graphical representations of the different statistical quantities of the calculated elevation residuals against the radius values of the DTM slope-based filter.

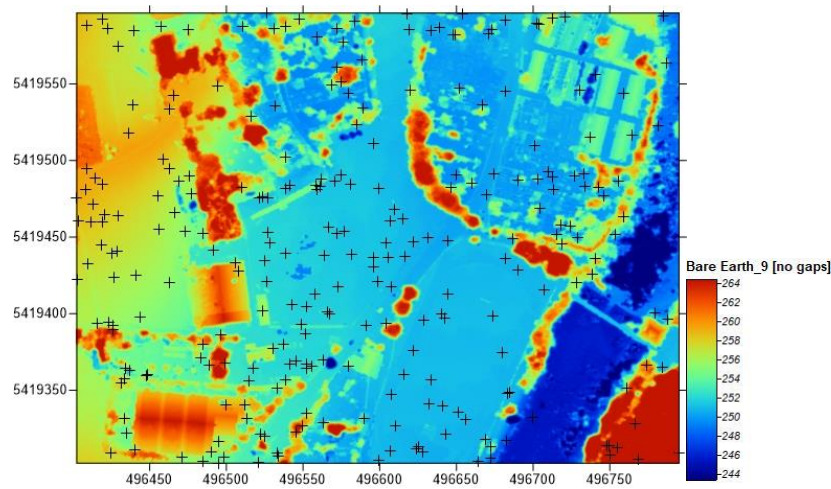


**Fig. 6.** Random distribution of the external check and ground truth points mapped over an aerial imagery DSM of the test area.

**Table 4.** Statistical analysis of the elevation residuals calculated from the closed gap bare earth models created through stripping off above ground objects from aerial imagery DSM with the use of the DTM slope-based filter of varying radii at the positions of the external checkpoints.

Slope filter radius (grid cells)	0	3	5	9	13	17	21	25	29	37
Max. residual (meters)	4.568	5.310	6.016	7.064	7.669	7.729	7.746	7.772	12.870	12.870
Min. residual (meters)	-9.029	-9.029	-9.026	-8.852	-8.852	-8.852	-8.852	-8.852	-8.852	-8.852
Range of residuals (meters)	13.597	14.339	15.042	15.916	16.521	16.581	16.598	16.624	21.722	21.722
Mean of residuals (meters)	-0.290	-0.211	-0.148	-0.073	-0.016	0.012	0.029	0.043	0.104	0.111
Median of residuals (meters)	0.029	0.035	0.041	0.045	0.046	0.048	0.052	0.052	0.055	0.055
Sum of residuals (meters)	-76.22	-55.57	-38.84	-19.27	-4.236	3.227	7.691	11.386	27.357	29.072
Standard deviation of residuals (meters)	1.571	1.568	1.615	1.626	1.604	1.598	1.594	1.595	1.785	1.792
Increase in the standard deviation of residuals (%)	0.0	-0.191	2.801	3.501	2.101	1.719	1.464	1.528	13.622	14.067
Standard Error of the mean (meters)	0.097	0.097	0.100	0.100	0.099	0.099	0.098	0.098	0.110	0.110

From **Table 4** and **Fig. 7A** the minimum, the mean and the median residual elevations increased slightly with the increase in the DTM slope-based filter radius. On the other hand, the maximum residual elevations and consequently the range of residual elevations increased with increasing the filter radius with small rates till radius of 25 grid cells where bigger increases in those two quantities occurred. Also, from table 4 and figure 7B fluctuated increases in the standard deviation of residuals of elevations occurred with increasing in the DTM slope-filter radius till filter radius of 25 grid cells where dramatic increases in the standard deviation of the residual elevations resulted referring to deterioration in the accuracy of the extracted elevations from the closed gap bare earth models that created with DTM slope-based filter of radius bigger than 25 grid cells. Thus, in the closed gap bare earth model created with the use of filter radius of 25 grid cells, the standard deviation of the residuals has increased by about 1.53%. On the other hand, in the closed gap bare earth model created with the use of filter radius of 29 grid cells the standard deviation of the elevation residuals has increased by 13.62%. This means rapid

deterioration of the bare earth model accuracy with increasing the filter size more than 25 grid cells. In this case DTM slope-based filter of radius size of 25 grid cells can be considered as the optimum filter.

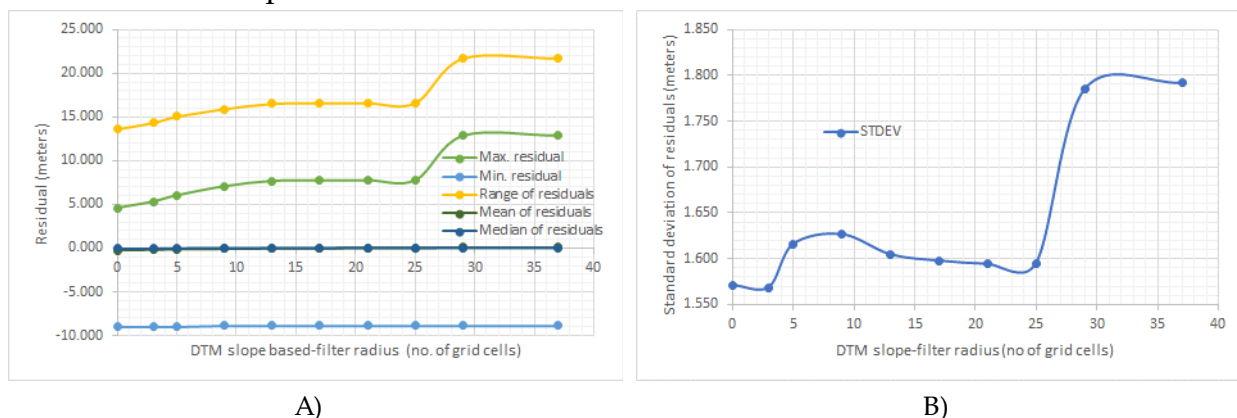


**Fig. 7.** A) Statistics of the residual elevations against the DTM slope-based filter radius, B) The standard deviation of the residual elevations against the DTM slope-based filter radius.

## CONCLUSIONS

For generation of a DTM all nonground cells must be eliminated from the DSM. Removal of the non-ground grid cells from the digital stereo pair DSMs can be performed through filtering operations. The DTM slope-based filter is one of the low pass filters which removes the grid cells of high slopes. This research aimed at assessment of the efficiency of the DTM slope-based filter in stripping off above ground objects from the digital aerial imagery DSMs for creation of reliable DTMs in rural landscape. The test area located at the west bank of a river at Vaihingen city, Germany possesses a variety of rural landscape features. A DSM of 0.09-meter ground resolution generated with the use of the dense matching approach has been used in the study. In this context, bare earth models and roughness layers created due to filtering the image matching DSM with the DTM slope-based filter at varying kernel radii in addition to closed gap bare earth models have been visually and statistically analyzed. Moreover, accuracy estimation of the closed gap bare earth models with external checkpoints of ground truth elevations have been undertaken. From the analysis the following points can be drawn:

- Gaps of no data have been left at the positions of the removed landscape where the amounts of the removed landscape increase with increases in the filter radius where the standard deviation of the bare earth model elevations has decreased by about 12% with the use of a filter of 37 grid cell radius.
- Concentrations and amounts of the removed landscape in the roughness layers increase with increasing the radius of the DTM slope-based filter that is expressed statistically as increases in the numbers of the data cells with decreases in the numbers of the no data cells due to increases in the filter radius.

- In the closed gap bare earth models continuous surfaces have been obtained, however, even with the use of large filter radii amounts of above ground features have yet to be removed referring to limitations of the DTM slope-base filter. However, in the closed gap models there are decreases in the mean, sum and standard deviation of elevations due to increases in the filter radius.
- In the closed gap bare earth model created with filter radius of 25 grid cells, the standard deviation of the elevation residuals has increased by only 1.53%. However, with filter radius of 29 grid cells that standard deviation has increased by 13.62% referring to rapid deterioration in the bare earth model accuracy with increasing the filter size more than 25 grid cells.
- More investigation may be necessary for better removal of the above ground features from the DSM with the use of the DTM slope-based filter where application of iterative processing could be more effective in removal of above ground features.

## ACKNOWLEDGEMENTS

“The Vaihingen data set was provided by the German Society for Photogrammetry, Remote Sensing and Geoinformation (DGPF) [29]”

The author would like to thank the two anonymous reviewers who provided constructive comments that helped strengthen the paper.

## References

- [1] Rokhmana, C. A., and Sastra, A. R., 2020. Filtering DSM extraction from Worldview-3 images to DTM using open source software. IOP Conf. Ser.: Earth Environ. Sci. 500 012054.
- [2] Stereńczak, K., Ciesielski, M., Balazy, R. & Zawila-Niedźwiecki, T., 2016. Comparison of various algorithms for DTM interpolation from LIDAR data in dense mountain forests. *European Journal of Remote Sensing*, 49:1, 599-621.
- [3] Zhao, Z., Wang, H., Wang, C., Wang, S., Li, Y. 2019. Fusing LiDAR Data and Aerial Imagery for Building Detection Using a Vegetation-Mask-Based Connected Filter. *IEEE Geoscience and Remote Sensing Letters*. PP. 1-5. 10.1109/LGRS.2019.2894896.
- [4] Luethje, F., Tiede, D., Eisank, C., 2017. Terrain Extraction in Built-Up Areas from Satellite Stereo-Imagery-Derived Surface Models: A Stratified Object-Based Approach. *ISPRS Int. J. Geo-Information*, 6, 9; doi:10.3390/ijgi6010009.
- [5] Balenović, I., Marjanović, H., Vuletić, I., Paladinić, E., Sever, M., Indir, K., 2015. Quality Assessment of High Density Digital Surface Model over Different Land Cover Classes. *Periodicum Biologorum, UDC 57:61, Vol 117, No 4, 2015*.
- [6] Dibs, H. and Al-Ansari, N., 2023. Integrating Highly Spatial Satellite Image for 3D Buildings Modelling Using Geospatial Algorithms and Architecture Environment. *Engineering*, 15, 220-233, <https://doi.org/10.4236/eng.2023.154017>.

- [7] Mikhail, E. M., Bethel, J. S. and McGlone, C. J., 2001. Introduction To Modern Photogrammetry. John Wiley & Sons, Inc.
- [8] Lillesand, T. M. and Keifer, R. W., 2015. Remote Sensing and Image Interpretation. seventh Edition, John Wiley & Sons, Inc.
- [9] Schenk, T., 1999. Digital Photogrammetry. Volume I, TerraScience, 16218 Bailor Rd., Laureville, OH 43135.
- [10] Karel, W., Pfeifer, N., Briese, C. 2006. DTM quality assessment. Commission II Symposium. Vienna; 12-14 July, 2006. International Archives of ISPRS, XXXVI/2, 1682-1750: 7 -12.
- [11] Silva CA, Klauberg C, Hentz ÂMK, Corte APD, Ribeiro U, Liesernberg V., 2018. Comparing the Performance of Ground Filtering Algorithms for Terrain Modeling in a Forest Environment Using Airborne LiDAR Data . Floresta e Ambiente 2018; 25(2): e20160150
- [12] Yadav, Y., Kushwaha, S., Mokros, M., Chudá, J., Pondelík, M. 2023. Integration of iPhone LiDAR With Quadcopter and Fixed Wing UAV Photogrammetry For The Forestry Applications. The International Archives of the Photogrammetry, Remote Sensing and Spatial Information Sciences, Volume XLVIII-1/W3-2023.
- [13] Pijl, A., Bailly, J.S., Feurer, D., El Maaoui, M.A.; Boussema, M.R.; Tarolli, P. 2020. TERRA: Terrain extraction from elevation rasters through repetitive anisotropic filtering. International Journal of Applied Earth Observation Geoinformation, 84, 101977.
- [14] Štroner, M.; Urban, R.; Lidmila, M.; Kolář, V.; Křemen, T. 2021. Vegetation filtering of a steep rugged terrain: The performance of standard algorithms and a newly proposed workflow on an example of a railway ledge. Remote Sensing 13, 3050.
- [15] Gevaert, C.; Persello, C.; Nex, F.; Vosselman, G. 2018. A deep learning approach to DTM extraction from imagery using rule-based training labels. ISPRS Journal of Photogrammetry and Remote Sensing, 142, 106–123.
- [16] Rashidi, P., and Rastiveis, H., 2018. Extraction of ground points from LiDAR data based on slope and progressive window thresholding (SPWT). Earth Observation and Geomatics Engineering 2(1) (2018) 36–44.
- [17] Krauß, T., Arefi, H., Reinartz, P. 2011. Evaluation of selected methods for extracting digital terrain models from satellite born digital surface models in urban areas. SMPR2011, 18.-19. May 2011, Tehran, Iran.
- [18] Özcan, A. H., Ünsalan, C. & Reinartz, P. 2018. Ground filtering and DTM generation from DSM data using probabilistic voting and segmentation, International Journal of Remote Sensing, 39:9, 2860-2883, DOI: 10.1080/01431161.2018.1434327.

- [19] Arefi, H., d'Angelo, P., Mayer, H. and Reinartz, P., 2011. Iterative approach for efficient digital terrain model production from CARTOSAT-1 stereo images. *Journal of Applied Remote Sensing* 053527-1 Vol. 5, 2011.
- [20] Höhle, J., Øster Pedersen, C., Bayer, T., & Frederiksen, P., 2010. The Photogrammetric Derivation of Digital Terrain Models in Built-up Areas. *Photogrammetric Journal of Finland*, 22(1), 33-45.
- [21] Perko, R., Raggam, H., Gutjahr, KH., Schardt. M., 2015. Advanced DTM Generation from Very High-Resolution Satellite Stereo Images. *ISPRS Annals of the Photogrammetry, Remote Sensing and Spatial Information Sciences*, Volume II-3/W4, 2015 PIA15+HRIGI15 – Joint ISPRS conference 2015, 25–27 March 2015, Munich, Germany.
- [22] Song, H.; Jung, J. 2023. An Object-Based Ground Filtering of Airborne LiDAR Data for Large-Area DTM Generation. *Remote Sensing*, 15, 4105. <https://doi.org/10.3390/rs15164105>.
- [23] Kang, C.; Lin, Z.; Wu, S.; Lan, Y.; Geng, C.; Zhang, S. 2023. A Triangular Grid Filter Method Based on the Slope Filter. *Remote Sensing*, 15, 2930.
- [24] Wichmann, V. 2010. Module DTM Filter (slope-based). SAGA-GIS Module Library Documentation (v2.2.5). Available from: [http://www.saga-gis.org/saga\\_tool\\_doc/2.2.5/grid\\_filter\\_7.html](http://www.saga-gis.org/saga_tool_doc/2.2.5/grid_filter_7.html).
- [25] Vosselman, G. and Maas, H.G. 2001. Adjustment and filtering of raw laser altimetry data. *Proceedings of OEEPE Workshop on Airborne Laserscanning and Interferometric SAR for Detailed Digital Terrain Models*.
- [26] Vosselman, G. 2000. Slope based filtering of laser altimetry data. *IAPRS*, Vol. XXXIII, Part B3, Amsterdam, The Netherlands. pp.935-942.
- [27] Lemaire, C., 2008. Aspects of the DSM production with high resolution images. *International Archives of the Photogrammetry, Remote Sensing and Spatial Information Sciences*, 37(B4), pp. 1143-1146.
- [28] Haala, N., Hastedt, H., Wolf, K., Ressel, C., Baltrusch, S., 2010. Digital photogrammetric camera evaluation – generation of digital elevation models. *Photogrammetrie – Fernerkundung – Geoinformation* 2(2010):99-115.
- [29] Cramer, M., 2010. The DGPF test on digital aerial camera evaluation – overview and test design. *Photogrammetrie – Fernerkundung – Geoinformation* 2(2010):73-82.
- [30] Rottensteiner, F., Sohn, G, Gerke, M., Wegner, J. D. 2013. ISPRS Test Project on Urban Classification and 3D Building Reconstruction. *ISPRS - Commission III - Photogrammetric Computer Vision and Image Analysis, Working Group III / 4 - 3D Scene Analysis*, <http://www.commission3.isprs.org/wg4/>.